The EMBO Journal (2008) 27, 1502–1512 | © 2008 European Molecular Biology Organization | Some Rights Reserved 0261-4189/08
www.embojournal.org

THE EMBO JOURNAL

EMBO open

Histone methyltransferase Dot1 and Rad9 inhibit single-stranded DNA accumulation at DSBs and uncapped telomeres

Federico Lazzaro[1,4], Vasileia Sapountzi[2,4], Magda Granata[1], Achille Pellicioli[1], Moreshwar Vaze[3,5], James E Haber[3], Paolo Plevani[1,*], David Lydall[2,*] and Marco Muzi-Falconi[1,*]

[1]Dipartimento di Scienze Biomolecolari e Biotecnologie, Universita' degli Studi di Milano, Milano, Italy, [2]Centre for Integrated Systems Biology of Ageing and Nutrition, Institute for Ageing and Health, Henry Wellcome Laboratory for Biogerontology Research, Newcastle University, Newcastle upon Tyne, UK and [3]Rosenstiel Basic Medical Sciences Research Center, Brandeis University, Waltham, MA, USA

Cells respond to DNA double-strand breaks (DSBs) and uncapped telomeres by recruiting checkpoint and repair factors to the site of lesions. Single-stranded DNA (ssDNA) is an important intermediate in the repair of DSBs and is produced also at uncapped telomeres. Here, we provide evidence that binding of the checkpoint protein Rad9, through its Tudor domain, to methylated histone H3-K79 inhibits resection at DSBs and uncapped telomeres. Loss of *DOT1* or mutations in *RAD9* influence a Rad50-dependent nuclease, leading to more rapid accumulation of ssDNA, and faster activation of the critical checkpoint kinase, Mec1. Moreover, deletion of *RAD9* or *DOT1* partially bypasses the requirement for CDK1 in DSB resection. Interestingly, Dot1 contributes to checkpoint activation in response to low levels of telomere uncapping but is not essential with high levels of uncapping. We suggest that both Rad9 and histone H3 methylation allow transmission of the damage signal to checkpoint kinases, and keep resection of damaged DNA under control influencing, both positively and negatively, checkpoint cascades and contributing to a tightly controlled response to DNA damage.

The EMBO Journal (2008) **27,** 1502–1512. doi:10.1038/emboj.2008.81; Published online 17 April 2008
Subject Categories: genome stability & dynamics
Keywords: chromatin; DNA damage checkpoint; DNA repair; histone methylation; telomeres

*Corresponding authors. P Plevani and M Muzi-Falconi, Dipartimento di Scienze Biomolecolari e Biotecnologie, Universita' degli Studi di Milano, Via Celoria 26, Milano 20133, Italy. Tel.: +39 02 50315034; Fax: +39 02 50315044; E-mail: marco.muzifalconi@unimi.it or D Lydall, Centre for Integrated Systems Biology of Ageing and Nutrition, Institute for Ageing and Health, Henry Wellcome Laboratory for Biogerontology Research, Newcastle University, Newcastle upon Tyne NE4 5PL, UK. Tel.: +44 191 256 3449; Fax: +44 191 256 3445; E-mail: d.a.lydall@ncl.ac.uk
[4]These authors contributed equally to this work
[5]Present address: Boston Biomedicals Inc., Norwood, MA 0206, USA

Received: 2 February 2008; accepted: 26 March 2008; published online: 17 April 2008

Introduction

Eukaryotic cells evolved a complex system to protect the genome from spontaneous and exogenous DNA damage. A central role is played by DNA damage checkpoint pathways, signal transduction cascades coordinating DNA replication, repair and recombination with cell cycle progression. The defining feature of an active checkpoint is the arrest of cell proliferation at the G1/S or G2/M transitions, or the slowing down of DNA replication (Elledge, 1996; Nyberg *et al*, 2002). Many details of the DNA damage checkpoint have been established using genetic and biochemical approaches in budding and fission yeast; the basic checkpoint response has been shown to be conserved in other eukaryotes (Longhese *et al*, 1998; Melo and Toczyski, 2002; Rouse and Jackson, 2002; Lydall and Whitehall, 2005). In budding yeast, it has been useful to examine the roles of checkpoint proteins at uncapped telomeres and unrepaired double-strand breaks (DSBs). Several repair, recombination and checkpoint factors are recruited at a DSB site, according to a well-established order (Lisby *et al*, 2004). DSB ends are initially processed to generate long 3′ single-stranded DNA (ssDNA) tails. The Mre11, Rad50, Xrs2 (MRX) complex is involved in this process, as mutations in the corresponding genes reduce the resection rate (White and Haber, 1990; Ivanov *et al*, 1994; Lee *et al*, 1998). However, MRX is not likely to be the nuclease itself: point mutations within Mre11 catalytic site do not affect resection of DSB ends (Moreau *et al*, 1999; Lee *et al*, 2002; Llorente and Symington, 2004). The nature of the nuclease(s) involved in DSB processing has been elusive; moreover, we lack information on the regulatory mechanisms governing DNA end resection (see Harrison and Haber, 2006 for a recent review). It has been recently shown that, both in human cells and in *Schizosaccharomyces pombe*, CtIP, a partner of the MRN complex, is required for efficient resection of DSB ends (Limbo *et al*, 2007; Sartori *et al*, 2007). In budding yeast, CtIP seems to correspond to Sae2, which also has a positive function in DSB processing (Clerici *et al*, 2005; Sartori *et al*, 2007). Recent studies show that CDK1 kinase is important for the generation of ssDNA tails; in fact, inhibition of CDK1 strongly interferes with resection (Aylon *et al*, 2004; Ira *et al*, 2004). ssDNA is bound by the RPA heterotrimer, generating a structure important for recruiting checkpoint factors (Kornbluth *et al*, 1992; Zou and Elledge, 2003; Zou *et al*, 2003; Majka *et al*, 2006).

PI3-like kinases have essential functions in checkpoint signal transduction in all eukaryotes. In budding yeast, the Mec1/Ddc2 checkpoint protein kinase is stimulated both by binding to RPA-coated ssDNA and by the checkpoint sliding clamp (Rad17, Mec3 and Ddc1) (Zou and Elledge, 2003; Zou

et al, 2003; Majka *et al*, 2006). Mec1 phosphorylates several targets, among these Ddc2, Ddc1, Rad9 and the protein kinases Chk1 and Rad53. Rad9 is a checkpoint adaptor molecule, linking the upstream Mec1 kinase with downstream Rad53 and Chk1 kinases, and it is essential for checkpoint function (Sanchez *et al*, 1996; Gardner *et al*, 1999; Blankley and Lydall, 2004). It is thought that Mec1-dependent phosphorylation of Rad9 recruits and catalyses Rad53 activation (Gilbert *et al*, 2001; Sweeney *et al*, 2005).

As well as being essential for cell cycle arrest, Rad9 contributes to DNA damage metabolism because Rad9 inhibits the accumulation of ssDNA at uncapped telomeres (Lydall and Weinert, 1995). This effect of Rad9 is not simply checkpoint signal transduction dependent, because other checkpoint proteins, such as Rad24, are also required to signal cell cycle arrest at uncapped telomeres and yet have the opposite resection phenotype (Lydall and Weinert, 1995). However, so far, no biochemical mechanism by which Rad9 inhibits resection at uncapped telomeres has been discovered. In addition, it was not known whether Rad9 inhibits ssDNA accumulation at other types of lesion, such as DSBs.

Budding yeast Rad9 interacts with the methylated K79 residue of histone H3, through the Rad9 Tudor domain, and this interaction regulates Rad9 function after DNA is damaged (Giannattasio *et al*, 2005; Wysocki *et al*, 2005; Grenon *et al*, 2007). Similar results were reported for *S. pombe* Crb2, where the binding target seems to be methylated H4-K20 (Sanders *et al*, 2004; Du *et al*, 2006), whereas for human 53BP1 binding to both residues has been reported (Huyen *et al*, 2004; Botuyan *et al*, 2006). Loss of methylation of the K79 residue of histone H3 impairs Rad9 phosphorylation and activation of Rad53, after DNA damage in G1 cells. Furthermore, a *rad9Y798Q* point mutation within the Tudor domain prevents Rad9 binding to chromatin and Rad9 hyper-phosphorylation after DNA damage (Giannattasio *et al*, 2005; Wysocki *et al*, 2005; Grenon *et al*, 2007; Hammet *et al*, 2007, and Supplementary Figure 1). The simplest explanation for these data is that methylated histone H3-K79 is involved in recruiting Rad9 to damaged chromosomes and that this contributes to Rad9 hyper-phosphorylation and checkpoint activation.

As H3-K79 appears to be constitutively methylated by the Dot1 methyltransferase in undamaged cells (90% of H3 is methylated at K79; van Leeuwen *et al*, 2002), it has been proposed that the critical event for Rad9 recruitment may be a DNA-damage-induced change in the status of chromatin, allowing exposure of this methylated residue (Huyen *et al*, 2004). Another intriguing option would be that Rad9 is always weakly bound to methylated H3-K79; upon damage Rad9 oligomerization may cause its accumulation at the sites of lesion. Moreover, post-translational modifications may induce changes in Rad9-binding mode and allow it to interact with other partners (Du *et al*, 2006; Hammet *et al*, 2007).

Here, we produce evidence that the interaction between histone H3-K79 and Rad9 inhibits accumulation of ssDNA at DSBs and at uncapped telomeres. This mechanism, requiring methylation of histone H3 and the Tudor domain of Rad9, regulates resection and appears to represent a strategy that coordinates cell cycle arrest with nuclease progression, thus limiting the amount of ssDNA generated during the cellular response to DNA damage.

Results

Methylation of H3-K79 controls Mec1 kinase activation after DNA damage

Dot1 is required for the G1/S DNA damage checkpoint (Giannattasio *et al*, 2005; Wysocki *et al*, 2005). To investigate the effect of the loss of *DOT1* on Mec1 kinase activity directly, we analysed the phosphorylation of its proximal target Ddc2, after DNA damage. Ddc2 is a stable partner of Mec1 and is directly phosphorylated by Mec1 *in vivo* and *in vitro* (Paciotti *et al*, 2000; Rouse and Jackson, 2000; Wakayama *et al*, 2001). Cells were arrested in G1 to avoid complications due to cell cycle-dependent phosphorylation of Ddc2 during the S/G2 phases (Paciotti *et al*, 2000). Analogous experiments in G2-arrested cells gave comparable results (Supplementary Figure 2). Surprisingly, in time-course analyses, we observed an increase in the phosphorylated form of Ddc2 in *dot1*Δ cells. G1-arrested wild-type (WT) and *dot1*Δ cells, expressing HA-tagged Ddc2, were treated with zeocine, which induces DSBs, and Ddc2 phosphorylation was evaluated at different times after the treatment. We consistently found that *dot1*Δ cells showed a hyper-modification of Ddc2, after induction of DSBs (Figure 1A and B). To verify that the increase in Ddc2 phosphorylation was due to Mec1 and not to another kinase, we compared Ddc2 phosphorylation in WT, *dot1*Δ, *mec1-1* and *dot1*Δ *mec1-1* mutants. Figure 1C shows that all the phospho-Ddc2 signal, detectable in WT and *dot1*Δ cells, disappears when Mec1 is defective, demonstrating that the increase in Ddc2 phosphorylation observed in *dot1*Δ cells is indeed due to the Mec1 kinase. These results suggest that more Mec1–Ddc2 kinase complexes can be activated after DSB induction, in the absence of Dot1, and hence H3-K79 methylation.

Failure to recruit Rad9 to histone H3 leads to an increase in Mec1 activation

Previous reports suggested that Dot1-dependent methylation of H3-K79 is critical for docking Rad9 to damaged chromatin (Wysocki *et al*, 2005; Toh *et al*, 2006). To test whether impairment of Rad9 recruitment to histone H3 would, similarly to a *dot1*Δ mutation, lead to an increase in Mec1 activity, we introduced a *RAD9* allele carrying a Y798Q point mutation in its Tudor domain; this mutation prevents Rad9 recruitment to damaged DNA, damage-dependent phosphorylation of Rad9 and the activation of Rad53 (Wysocki *et al*, 2005; Grenon *et al*, 2007, and Supplementary Figure 1). The kinetics of Mec1 activation after DSB induction was analysed in *rad9Y798Q* and *rad9*Δ cells. Figure 1D shows that, similarly to what was found in a *dot1*Δ strain, cells completely lacking Rad9 or expressing *rad9Y798Q* exhibit faster Ddc2 phosphorylation after DSB induction; quantification of the phospho-Ddc2 form confirmed the observation (Figure 1E). Taken together, these results strongly suggest that loss of Rad9 binding to methylated H3-K79 leads to a faster and more robust activation of Mec1 kinase in response to DSBs.

A robust DNA damage checkpoint is not triggered by DSBs themselves, but rather by processed DNA ends, containing long stretches of ssDNA, which recruit Mec1–Ddc2 kinase complexes (White and Haber, 1990; Lydall *et al*, 1996; Lee *et al*, 1998; Usui *et al*, 2001; Harrison and Haber, 2006). Therefore, the Mec1 hyper-activation detected in *dot1*Δ and

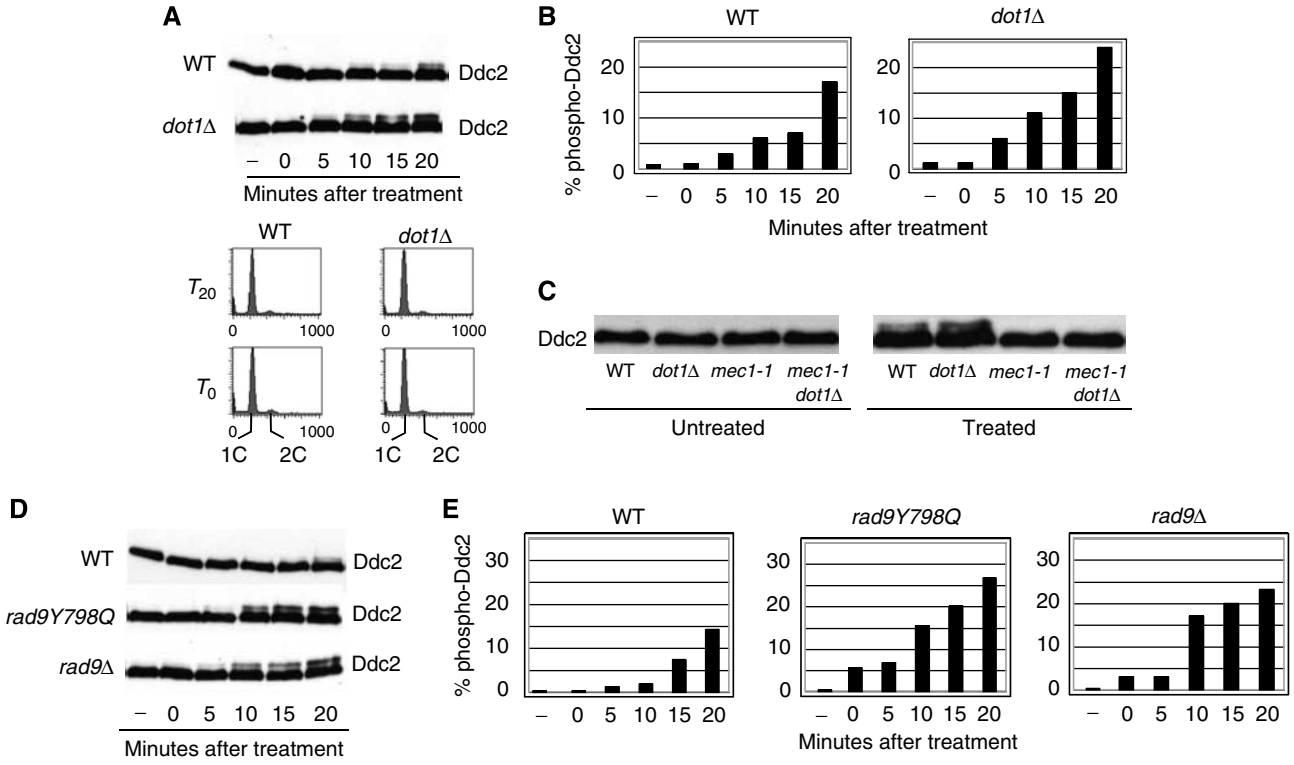

Figure 1 Loss of *DOT1* or *RAD9* leads to Mec1 kinase hyper-activation after induction of DSBs. (**A**) WT (YLL683.8/3b) and *dot1*Δ (YFL403/10b) cells carrying an HA-tagged version of *DDC2* at its chromosomal locus were arrested in G1 and treated with 50 μg/ml zeocine to induce DSBs. At the indicated times (–: untreated cells) samples were taken, protein extracts were prepared and the phosphorylation-dependent mobility shift of Ddc2 in SDS–PAGE was monitored by western blotting with 12CA5 antibodies (top panels). FACS profiles of the cultures (bottom panels) show that both cultures did not escape the G1 block throughout the experiment. (**B**) Quantification of the percentage of phosphorylated form relative to the total Ddc2 protein (from (A)). (**C**) Ddc2 phosphorylation was monitored in WT (YFL693), *dot1*Δ (YFL694), *mec1-1* (YFL219/9b), *mec1-1 dot1*Δ (YFL571.1) cells after treatment with zeocine, as in (A). (**D**) Western blots of Ddc2 in WT (YLL683.8/3b), *rad9Y798Q* (YFL502) and *rad9*Δ (YFL407/5a) cells, at different times after induction of DSBs. (**E**) Quantification of the bands from (D).

rad9 mutants could be explained if DSBs were more rapidly processed to ssDNA when Rad9 does not bind methylated H3.

Dot1 and Rad9 limit resection of DNA DSB ends

To test the hypothesis that more rapid activation of Mec1 kinase results from a faster production of ssDNA intermediates in *dot1*Δ, *rad9Y798Q* and *rad9*Δ cells, we investigated the kinetics of ssDNA formation after a single unrepairable DSB in these mutants, using an inducible HO endonuclease. Cells were arrested in G2, to prevent cell cycle-dependent effects on resection, and samples were collected at various time points after induction of the nuclease. ssDNA regions in genomic DNA were revealed by the loss of restriction sites distal to the HO-cut site, leading to the accumulation of uncut DNA fragments that were detected with a strand-specific probe, after alkaline electrophoresis (White and Haber, 1990; Shroff *et al*, 2004; Clerici *et al*, 2006. See Figure 2B for a map of the *MAT* locus and the location of probe used in these experiments). The kinetics of appearance of longer DNA fragments suggests that *dot1*Δ, *rad9Y798Q* and *rad9*Δ cells all showed more rapid resection than WT cells (Figure 2A). This finding was confirmed using a different assay where resection leads to the disappearance of a specific DNA restriction fragment in Southern blots (see Figures 5 and 6). These data suggest that the impairment of Rad9 binding to methylated H3-K79, as seen in *rad9*Δ, *rad9Y798Q*, *dot1*Δ and *rad9Y798Q dot1*Δ (not shown), leads to faster resection at an HO-induced DSB.

Dot1 and Rad9 control DNA processing at uncapped telomeres

The results reported so far suggest that a complex containing methylated H3 and Rad9 on damaged DNA inhibits ssDNA accumulation at DSBs. Consistent with this interpretation, earlier studies showed that Rad9 inhibits the accumulation of ssDNA at uncapped telomeres (Lydall and Weinert, 1995; Zubko *et al*, 2004). To assess the role of methylated H3-K79, and its relationship with Rad9, at uncapped telomeres, we analysed both DNA processing and checkpoint activation in a *cdc13-1* mutant background. At temperatures higher than 26°C, *cdc13-1* cells accumulate ssDNA and block cell division at the G2/M checkpoint (Garvik *et al*, 1995).

We first examined whether, as found above at DSBs, Dot1 inhibited resection at uncapped telomeres. We used QAOS (quantitative amplification of ssDNA) (Booth *et al*, 2001; Zubko *et al*, 2006) to measure the accumulation of ssDNA in synchronous cultures of *dot1*Δ *cdc13-1* strains. A *bar1*Δ mutation was present in strains to ensure efficient G1 cell cycle arrest with alpha factor and a *cdc15-2* mutation was present to ensure that checkpoint-deficient cells did not initiate more than one round of DNA replication during the course of an experiment because at 36°C *cdc15-2* mutants arrest in late anaphase (Zubko *et al*, 2006). We measured

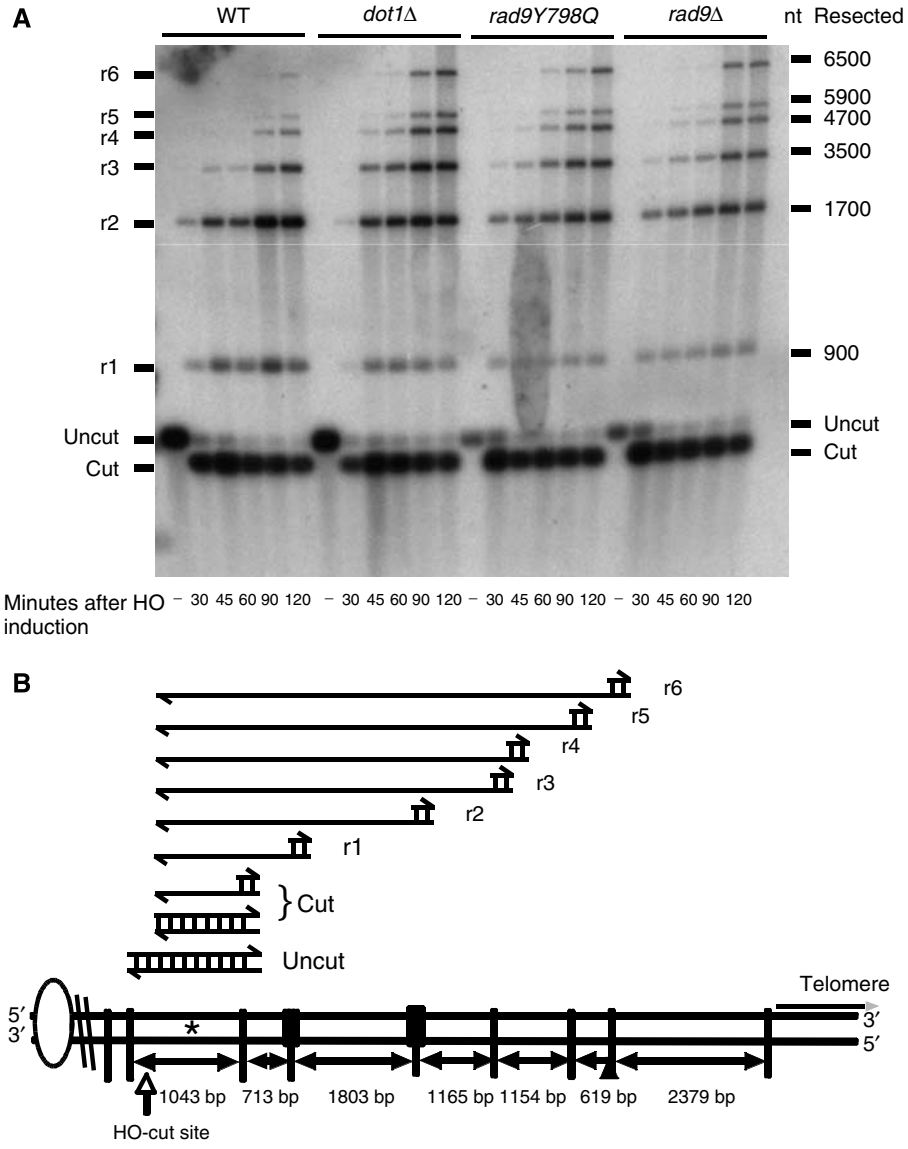

Figure 2 Resection of a DSB is faster in *dot1*Δ, *rad9Y798Q* and *rad9*Δ cells. (**A**) WT (JKM179), *dot1*Δ (YFL399), *rad9Y798Q* (YFL504) and *rad9*Δ (YFL419) cells, carrying a unique HO-cut site at the *MAT* locus and expressing the HO endonuclease under the inducible *GAL1* promoter, were grown in presence of lactate and arrested with nocodazole. HO was induced with galactose 2%. Genomic DNA, extracted from samples collected at the indicated times, was digested with *Ssp*I and separated on alkaline denaturating gels. Resection was monitored by Southern blotting using a ribo-probe specific for the 3′strand. (**B**) Scheme of the *MAT* locus**.** The figure shows the positions of the HO-cut site, and of the probe (asterisk) used for the experiments shown in (A). The black vertical bars indicate the *Ssp*I sites. The products of the digestion of differently resected molecules are shown above the scheme.

ssDNA at the *PDA1* locus, which lies about 30 kb away from the end of ChV-R (Figure 3A), because ssDNA does not accumulate at this locus in RAD^+ strains but does accumulate if Rad9 function is compromised (Figure 3B). As shown in Figure 3B, *dot1*Δ *cdc13-1* cells, similarly to *rad9*Δ *cdc13-1* strains, had significantly increased levels of ssDNA at *PDA1*, relative to *cdc13-1* strains suggesting that Dot1, similar to Rad9, protects subtelomeric DNA from nucleolytic degradation in *cdc13-1* mutants.

Dot1 affects checkpoint activation in response to telomere uncapping

As Dot1, the H3-K79 methylase, is important for activating Rad9 in response to DSBs (Giannattasio *et al*, 2005; Wysocki *et al*, 2005; Toh *et al*, 2006), we tested the checkpoint role of Dot1 after telomere uncapping. Impairing checkpoint pathways, for example *rad9*Δ, partially suppresses the temperature sensitivity of *cdc13-1* strains (Weinert *et al*, 1994; Zubko *et al*, 2004). Figure 4A shows that Dot1 inhibits growth of cells with uncapped telomeres because *dot1*Δ *cdc13-1* strains grow better than *cdc13-1* strains at 26.5°C. We note that *rad9*Δ *cdc13-1* strains grow better than *dot1*Δ *cdc13-1* strains. To test whether Dot1 growth inhibition of *cdc13-1* cells is mediated by the interaction of Rad9-Tudor domain with H3-K79^{me}, we analysed the effect of the *rad9Y798Q* mutation. Even though we routinely observed that *rad9Y798Q cdc13-1* strains grew better than *dot1*Δ *cdc13-1* strains, *rad9Y798Q cdc13-1* mutants behave most similarly to *dot1*Δ *cdc13-1* cells and grow better than *cdc13-1* cells but less well than *cdc13-1 rad9*Δ cells (Figure 4A). This can be explained if the

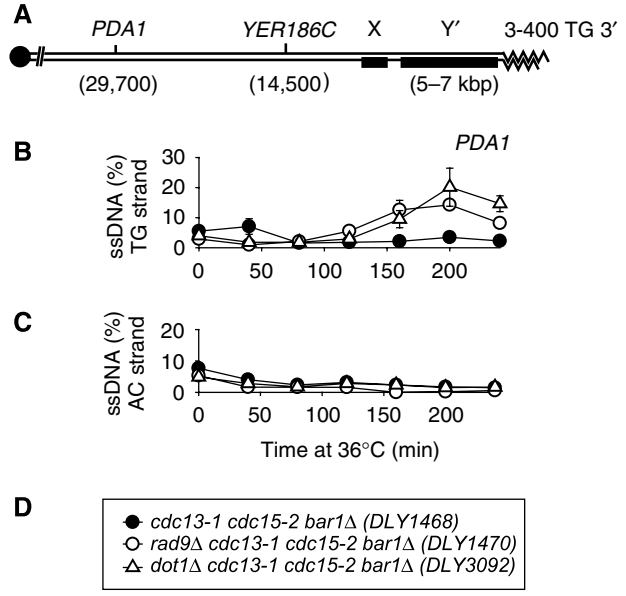

Figure 3 Dot1 protects subtelomeric DNA from degradation in *cdc13-1* mutants. (**A**) Schematic of ChrVR telomere. (**B**) Accumulation of ssDNA on the TG strand at *PDA1*. (**C**) Accumulation of ssDNA on the AC strand at *PDA1*. (**D**) Key to (B, C). In (B, C), ssDNA was measured by QAOS. A single representative experiment is shown with error bars indicating the error of the mean of three independent measurements of the same DNA samples, in most cases the error bars are small and are hidden by the symbols.

rad9Y798Q point mutation affects the structure of Rad9 or its interaction with other proteins. Moreover, loss of *DOT1* causes redistribution of the SIR factors and this could also influence the vitality of *cdc13-1* cells. The epistatic relationships between these mutations are shown in Supplementary Figure 3. Taken together, these data suggest that the role of Dot1 in responding to telomere uncapping is mediated by the Tudor domain of Rad9. However, our finding that *rad9Y798Q cdc13-1* and *dot1*Δ *cdc13-1* mutants do not grow as well as *cdc13-1 rad9*Δ strains, at semi-permissive temperature, suggests the existence of a Rad9-dependent mechanism acting independently of the H3-K79^{me}/Rad9 Tudor domain at uncapped telomeres.

Our observations suggest a role for H3-K79 methylation in checkpoint activation following telomere uncapping. To address this directly, single cells were monitored for their ability to form colonies at different temperatures (Figure 4B, and Supplementary Figure 4). Figure 4B plots the fraction of colonies that contain more than 20 cells for checkpoint and nuclease-deficient *cdc13-1* strains over a range of temperatures. The higher the temperature the smaller the colony size for both checkpoint-proficient and -deficient cells. At temperatures higher than 26°C, checkpoint proficient *cdc13-1* cells divide slowly and form smaller colonies than checkpoint- or nuclease-deficient strains (Figure 4B). At high levels of telomere uncapping, for example, 30°C and 36°C, the colonies of *dot1*Δ *cdc13-1* strains are of similar size as those of *cdc13-1*. At lower levels of uncapping, for example, 27°C

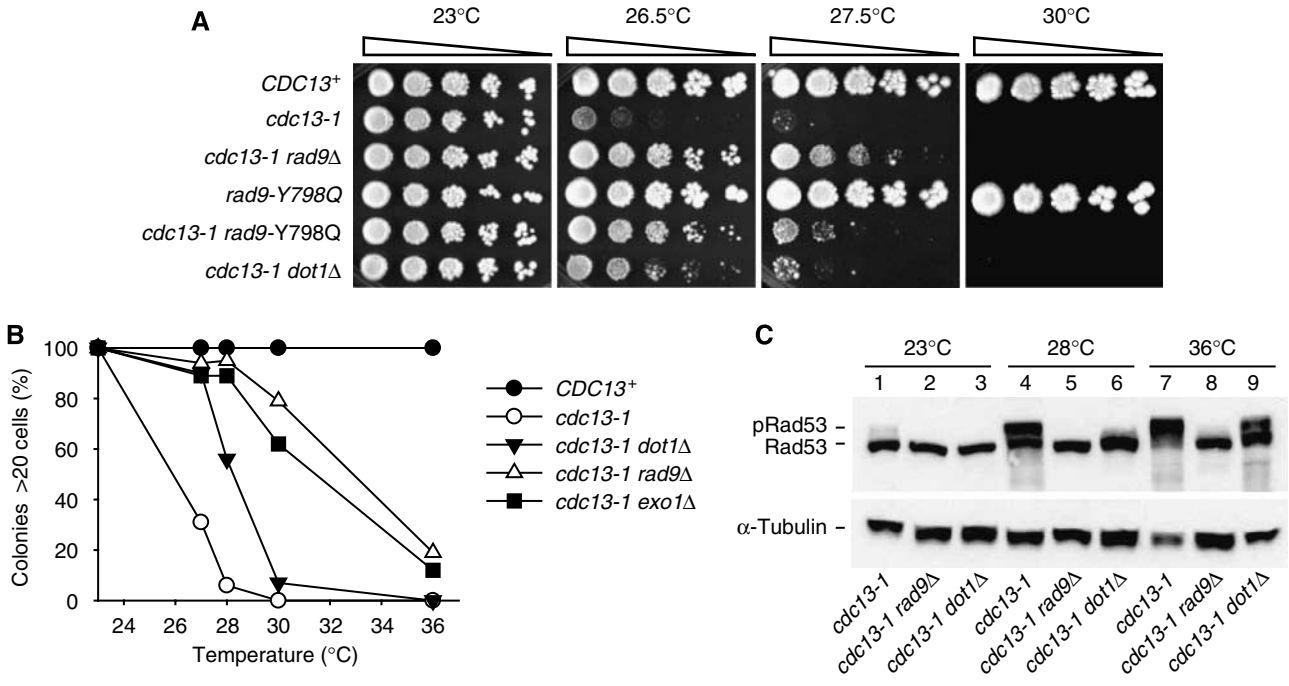

Figure 4 Dot1 contributes to checkpoint-dependent arrest of *cdc13-1* mutants. (**A**) Five-fold dilutions of strains with indicated phenotypes were spotted onto YEPD plates and grown for 3 days at the temperatures shown. Strains were *CDC13*$^{+}$ (DLY640), *cdc13-1* (DLY1195), *cdc13-1 rad9*Δ (DLY1256), *rad9-Y798Q* (YFL502), *cdc13-1 rad9-Y798Q* (DLY3083) and *cdc13-1 dot1*Δ (DLY2880). (**B**) Single cells were spread onto agar plates and colony formation of *CDC13*$^{+}$ (DLY640), *cdc13-1* (DLY1195), *cdc13-1 dot1*Δ (DLY2881) and *cdc13-1 rad9*Δ (DLY1256) cells was monitored after 20 h at temperatures shown (see Supplementary Figure 4). Number of colonies containing more than 20 cells is plotted against temperature. (**C**) Cultures of *cdc13-1* (DLY1195), *cdc13-1 rad9*Δ (DLY1256) and *cdc13-1 dot1*Δ (DLY2881) were grown at the indicated temperatures for 5 h and Rad53 levels in protein extracts were immunoblotted with anti-Rad53 antibodies or anti-tubulin antibodies, as a loading control.

and 28°C, *dot1*Δ *cdc13-1* cells form larger colonies than *cdc13-1* strains (Figure 4B). However, *dot1*Δ *cdc13-1* colonies are smaller than *cdc13-1 rad9*Δ cells at 27°C (Supplementary Figure 4). This, and the spots tests shown in Figure 4A, suggest that Dot1 has a partial function in checkpoint activation, a function that is only detectable at low levels of DNA damage. Consistent with this interpretation, we saw complete and efficient cell cycle arrest of *dot1*Δ *cdc13-1* mutants in the first cycle after G1 release in the ssDNA measurement experiment shown in Figure 3 (data not shown).

The role of Dot1 in checkpoint activation at intermediate temperatures was confirmed by measuring phosphorylation of Rad53. At 23°C, telomeres in *cdc13-1* strains are capped and Rad53 is largely hypo-phosphorylated (Figure 4C, lanes 1–3). In response to low levels of telomere uncapping (28°C), Rad53 is hyper-phosphorylated in a Dot1- and Rad9-dependent manner (Figure 4C, lanes 4–6). However, at higher levels of telomere uncapping (36°C) a significant fraction of Rad53 is hyper-phosphorylated in *dot1*Δ *cdc13-1* strains (Figure 4C, lane 9). These observations suggest that at low levels of telomere uncapping, Dot1 has a more important function in Rad9-dependent checkpoint activation that it does at higher levels of uncapping, when presumably alternative mechanisms ensure that Rad9 is activated.

Loss of Rad9 or Dot1 partially bypasses the requirement for CDK1 in DSB resection

The molecular mechanisms controlling DNA end resection at DSBs and uncapped telomeres are poorly understood. Recent reports showed that CDK1 activity is necessary to obtain effective resection, both at DSBs and uncapped telomeres (Aylon *et al*, 2004; Ira *et al*, 2004; Vodenicharov and Wellinger, 2006). Indeed, inhibition of CDK1, by overexpression of the inhibitor Sic1, leads to a notable reduction of 5′–3′ processing of DSB ends (Aylon *et al*, 2004; Ira *et al*, 2004, and Figure 5B). To understand the relationships between the Rad9-dependent and the CDK1-dependent mechanisms that regulate resection, we analysed the processing of a DSB in *rad9*Δ and *dot1*Δ cells after inhibition of CDK1 activity. We used a yeast strain where a site-specific DSB can be repaired by single-strand annealing (SSA) between two short regions of homology flanking the cut site (Figure 5A) (Sugawara *et al*, 2000; Vaze *et al*, 2002). We chose this system for analysis of resection because in this context we can follow simultaneously processing at sites close and far away from the DSB; moreover, we can monitor the appearance of the repair product, which being dependent upon the generation of ssDNA is also a measure of the velocity of resection. At various times after induction of the HO cut and after the concomitant induction of CDK1 inhibitor Sic1, we monitored both DNA end processing and DSB repair by SSA, through Southern blot analysis. Our data show that loss of *RAD9* or *DOT1* accelerates the appearance of the band corresponding to the repaired chromosome (the SSA product in Figure 5B); the repair product is clearly detectable 5 h after HO induction in WT cells, whereas it is already visible at the 3 h time point in the *rad9*Δ strain (Figures 5B and 6B). This confirms that absence of *RAD9* stimulates DSB resection and SSA and the results with *dot1*Δ argue that this effect partially depends upon H3-K79 methylation. Interestingly, whereas *SIC1* overexpression almost completely inhibits the generation of the SSA product in a WT background, loss of *RAD9* or *DOT1* significantly reduces the effect due to the inhibition of CDK1 (Figures 5B and 6B). This may suggest that the CDK1-dependent stimulation of resection could exert a function by overcoming the inhibitory effect of Rad9 bound to H3-K79^{me}.

As SSA-based DNA repair depends upon annealing of two complementary ssDNA, faster SSA product generation in this experiment agrees with the faster resection observed in the experiments described above (Figures 1 and 2), but a contribution by a more efficient recombination mechanism could not be excluded. To this aim, we tested the effect of *RAD9* deletion in the absence of the critical recombination protein Rad52. SSA is reduced >95% in the absence of Rad52. Figure 5C shows that resection in *rad52*Δ *rad9*Δ double mutant cells is accelerated, compared with *rad52*Δ cells. This is also confirmed by measuring resection of the *his4*::*leu2* fragment in Figure 5B (see quantifications in Figure 6A) and by monitoring resection of the HO-cut fragment in a yeast strain where the break cannot be repaired by SSA (Supplementary Figure 5). These results suggest that loss of *RAD9* most likely accelerates SSA DNA repair through a faster accumulation of ssDNA.

The identity of all the nucleases resecting DSB ends and uncapped telomeres has not yet been fully elucidated, but previous reports implicated the MRX complex and Exo1 in this process (Llorente and Symington, 2004; Harrison and Haber, 2006) as well as undefined nucleases, ExoX, ExoY (Zubko *et al*, 2004; Harrison and Haber, 2006). To help determine how Rad9 regulates resection at DSBs, we examined cells lacking Exo1 or Rad50. Figure 7 shows that loss of Rad9 causes an accelerated resection in the absence of Exo1, where the SSA product appears at the 3 h time point in a *rad9*Δ background and at the 6 h time point in a *RAD9* background. These results suggest that Exo1 is not required for the rapid rates of resection observed in *rad9*Δ strains. On the other hand, if *RAD50* is missing, there is no strong effect of the loss of *RAD9*, suggesting that Rad9 inhibits, at least in part, a *RAD50*-dependent nuclease (Figure 7). Similar conclusions can be drawn analysing resection at the distal site (Supplementary Figure 6).

Discussion

DNA damage checkpoint pathways are powerful intracellular signal transduction cascades that, following genomic lesions, inhibit cell cycle progression and coordinate DNA replication, repair and recombination with cell division. DNA damage checkpoint pathways are understood to be based on kinase-dependent signal transduction cascades stimulated by damaged DNA (Longhese *et al*, 1998; Lydall and Whitehall, 2005); in this context, Rad9, the first checkpoint protein to be identified, has been assigned a mediator function, necessary to link the upstream kinase, Mec1, with activation of the downstream kinases Rad53 and Chk1 (Gilbert *et al*, 2001; Blankley and Lydall, 2004; Sweeney *et al*, 2005).

Rad9 has recently been shown to bind to methylated K79 residue of histone H3 through the Rad9 Tudor domain and this interaction is important for the checkpoint role of Rad9 (Giannattasio *et al*, 2005; Wysocki *et al*, 2005). The finding that other Tudor domain checkpoint mediator proteins bind methylated histones suggests functional evolutionary conservation of the interactions between checkpoint proteins and

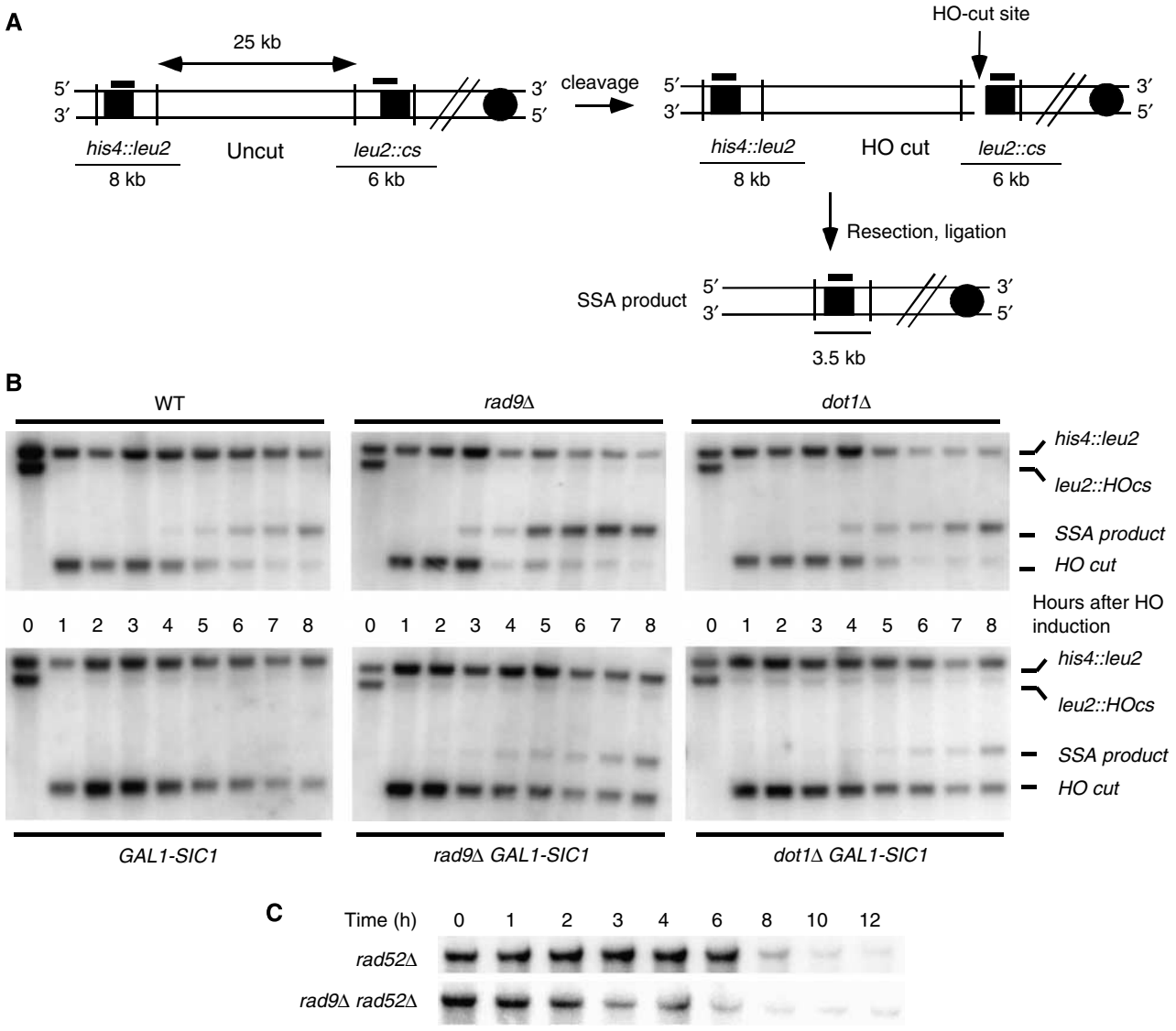

Figure 5 Loss of Rad9 bypasses CDK1 requirement for SSA and resection. (**A**) Map of the YMV80 Chr III region, containing the HO-cut site. Vertical bars show the relevant *Kpn*I sites. The thick lines above the map indicate the positions where the probe hybridizes. After HO cleavage, DNA is resected. When the left and right *leu2* sequences have been converted to ssDNA, repair by SSA can take place and can be monitored by the appearance of a SSA product in a Southern blot. (**B**) Exponentially growing YEP + raffinose cell cultures of WT (YMV80) and isogenic *rad9*Δ (Y31), *GAL1-SIC1* (Y20), *rad9*Δ *GAL1-SIC1* (Y293), *dot1*Δ (YFL736) and *dot1*Δ *GAL-SIC1* (YFL738) strains, carrying an HO-cut site and a gal-inducible HO gene, were arrested with nocodazole; galactose was added at time zero. *Kpn*I-digested DNA, prepared from cells collected at the indicated times, was analysed by Southern blotting with a *LEU2* probe. Two fragments, 8 and 6 kb long (*his4*::*leu2*, *leu2*::*HOcs*) are evident in the absence of HO cut, whereas the HO-induced DSB causes the disappearance of the 6-kb species and the formation of a 2.5-kb fragment (HO-cut fragment). Repair by SSA converts such fragment to a repair product of 3.5-kb (SSA product). (**C**) Speed of resection was evaluated in *rad52*Δ (YMV037) and *rad52*Δ *rad9*Δ (YMV038) cells under similar conditions by monitoring the disappearance of the *his4*::*leu2* signal.

modified histones; in fact, mammalian 53BP1 and *S. pombe* Crb2p interact with methylated H4-K20 (Sanders *et al*, 2004; Botuyan *et al*, 2006; Du *et al*, 2006). We show here that Dot1, the H3-K79 methylase, and the Tudor domain of Rad9, also have a negative feedback function in the checkpoint response to DSBs, where they inhibit processing of DSB ends and activation of the Mec1 kinase. By analysing the extent of phosphorylation of Ddc2, the most proximal target of Mec1, after induction of DSBs, we observed that loss of methylation of H3-K79 leads to more rapid activation of Mec1 and to an increase in the level of phosphorylated species. Methylation of histone H3 in nucleosomes, similar to histone tail acetylation, could alter chromatin structure directly or influence susceptibility to nucleases, affecting Mec1 activation. On the other hand, Dot1-dependent methylation of H3 could help in the recruitment of other factors, such as Rad9, that may influence Mec1 activity. Indeed, a mutation affecting Rad9 Tudor domain or a deletion of *RAD9*, also caused hyper-activation of Mec1, strongly suggesting that H3-K79 interaction with Rad9 is important to limit Mec1 activation. Moreover, although both the Rad9 Tudor domain and Dot1 contribute to the checkpoint response at low levels of telomere uncapping, they are not necessary at high levels of telomere uncapping.

Much of what we know on the mechanisms involved in activation of Mec1 derives from studying the response to site-specific DSBs. The DNA ends generated by the cleavage are processed by nucleolytic activities, which leave long tails of

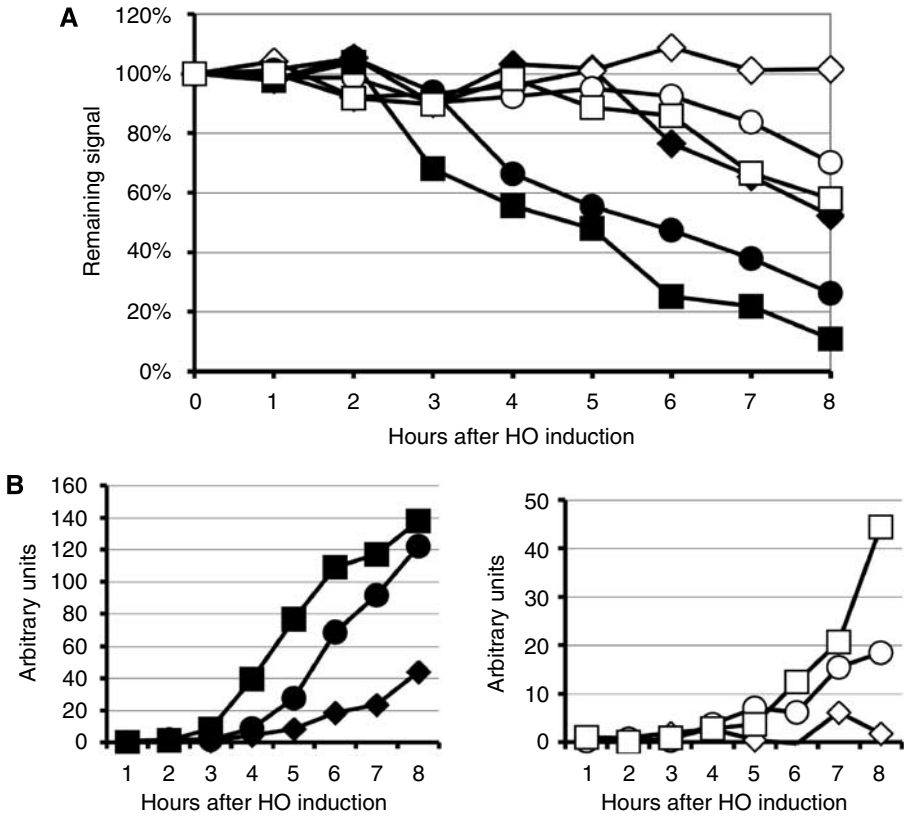

Figure 6 Loss of *RAD9* or *DOT1* increase resection at DSBs bypassing the requirement for Cdk1. The graphs represent quantifications of data shown in Figure 5. (**A**) Quantification of the *his4*::*leu2* band, measuring resection at the distal site. The intensity of each band was normalized with respect to loading. The signal present before HO cutting was set to 100%. (**B**) Quantification of the SSA product band. ■ *rad9*Δ; □ *rad9*Δ *GAL-SIC1*; ● *dot1*Δ; ○ *dot1*Δ *GAL-SIC1*; ◆ WT; ◇ WT *GAL-SIC1*.

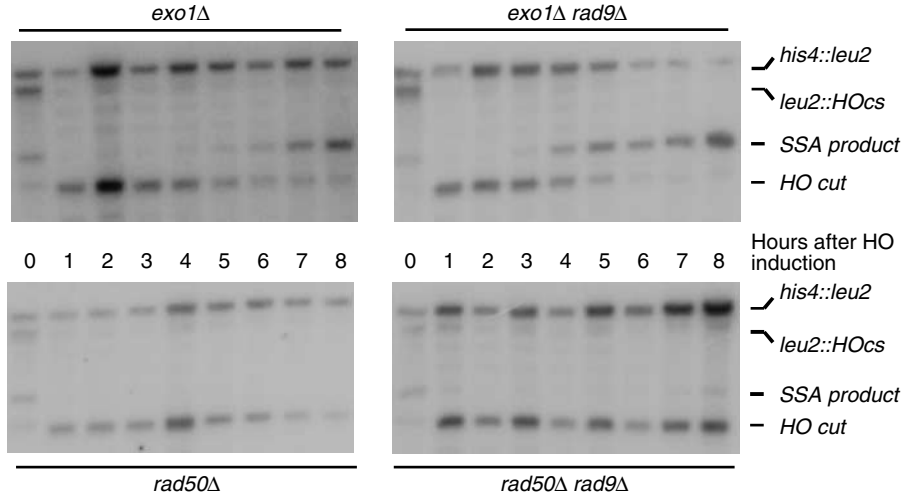

Figure 7 Fast resection in the absence of Rad9 depends upon *RAD50*. SSA was analysed in *exo1*Δ (Y28), *exo1*Δ *rad9*Δ (YFL802), *rad50*Δ (YFL827) and *rad50*Δ *rad9*Δ (YFL809) using Southern blotting as described in Figure 5.

ssDNA (see Harrison and Haber, 2006 for a review). RPA-covered ssDNA appears to be a prerequisite for Mec1 activation (Zou and Elledge, 2003; Zou *et al*, 2003). Therefore, we evaluated the effect of Dot1 and Rad9 on the amount of ssDNA generated after a site-specific DSB. Our data show that various genetic manipulations expected to cause loss of Rad9 binding to histone H3 lead to an increase in the speed of resection both at DSBs and uncapped telomeres, suggesting that chromatin-bound Rad9 could represent a functional or physical barrier to exonucleolytic processing of DSBs and uncapped telomeres.

How does the Rad9 H3-K79 interaction affect ssDNA accumulation at telomeres and DSBs? The question is difficult to address at this stage because important details about the mechanisms by which ssDNA is generated are lacking. For example, the nucleases responsible for generating ssDNA

have not been fully defined yet, although there are roles for Exo1, MRX and other nuclease activities (Llorente and Symington, 2004; Zubko *et al*, 2004; Harrison and Haber, 2006). Moreover, the requirement for CDK1 activity in DSB processing suggests that CDK1 may target a protein involved in resection (Aylon *et al*, 2004; Ira *et al*, 2004). In *S. pombe* the Rad9 orthologue, Crb2, mediates the effect of CDK1 on DSB repair (Caspari *et al*, 2002). Moreover, phosphorylation by CDK1 allows Crb2 to bind close to DSBs through the interaction with Cut5, the orthologue of Dpb11, and this suffices for activating the DNA damage response to DSB (Du *et al*, 2006). To better define the mechanisms controlling nucleolytic processing of DSBs, we investigated the effect of CDK1 inhibition on resection in the absence of *RAD9*. Our data show that deletion of *RAD9* makes resection much less sensitive to CDK1 inhibition; a similar, albeit reduced, effect is detected in the absence of Dot1, suggesting that binding to methylated H3-K79 is a critical regulatory process. A likely explanation for this result is that one major requirement for CDK1 in DSB processing relies on the removal of Rad9-dependent inhibition of resection, even though a direct effect on some nuclease or other factors cannot be excluded. It is interesting that Rad9 has been shown to be phosphorylated by CDK1 (Ubersax *et al*, 2003; Grenon *et al*, 2007) and this may modulate chromatin accessibility by nucleases.

Intriguingly, the inhibitory effect of Rad9 on resection is most evident when monitoring the disappearance of a DNA fragment far away from a DSB or uncapped telomere, compared with regions closer to the primary lesion (Supplementary Figure 7, and Zubko *et al*, 2004). These observations, together with the residual inhibition by *GAL-SIC1* in *rad9*Δ cells (Figure 5B), suggest that a different CDK1 target could be involved in controlling resection initiation, whereas Rad9 may be limiting the speed and amount of DNA processing. This hypothesis would be consistent with recent findings, reporting an important role for CtIP in the control of DSB resection (Limbo *et al*, 2007; Sartori *et al*, 2007).

Further attempts to define the mechanism confirm that Exo1- and Rad50-dependent nucleases participate in resecting DSBs and suggest that the observed Rad9-dependent inhibition affects in part or in whole *RAD50*-dependent nuclease activity. In contrast, at uncapped telomeres MRX is not responsible for generating ssDNA, this function can be ascribed to unidentified nucleases (ExoX, ExoY) (Foster *et al*, 2006). Importantly, high levels of ssDNA accumulation after telomere uncapping in *exo1*Δ *rad9*Δ double mutants indicate that Rad9-dependent inhibition of ssDNA production may be a general aspect of the DNA damage response (Zubko *et al*, 2004). Notably, the only transcriptional change caused by deletion of *DOT1*, and therefore induced by loss of H3-K79 methylation, is overexpression of Y′ repeats, which are found at the telomeres (van Leeuwen *et al*, 2002). It has been postulated that this is because, in the absence of H3-K79 methylation, the Sir2 histone deacetylase moves from its normal location at telomeres to spread more evenly around the genome. This movement correlates with a loss of the heterochromatic status at telomeres and may be responsible, in part, for the enhanced resection at uncapped telomeres in *dot1* and *rad9* mutants.

Figure 8 summarizes possible mechanisms by which the Rad9 H3-K79 interaction may affect ssDNA accumulation at DSBs and telomeres: Rad9, when bound to chromatin, may represent a direct structural impediment to nuclease activity or it may promote the formation of a chromatin structure that inhibits exonucleolytic processing of DNA. This could be, in part or completely, due to the interaction of the Tudor domain of Rad9 with methylated H3. But other interactions between Rad9 and chromatin may also contribute to inhibiting nuclease activity; for example, the BRCT domain of Rad9 may interact with phosphorylated checkpoint proteins, or histones, at sites of DNA damage and inhibit nuclease activity (see Du *et al*, 2006; Hammet *et al*, 2007). Consistent with the idea of Rad9 affecting nuclease activity by more than one chromatin interaction, yeast strains defective in H3-K79 methylation are not as defective at inhibiting resection as *rad9*Δ mutants.

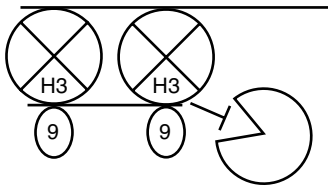

Figure 8 Potential mechanisms for the role of Rad9 in resection inhibition in response to DSBs and uncapped telomeres. Rad9 bound to the methylated H3-K79 interferes with the action of the nuclease(s) or generates a non permissive chromatin configuration.

The eukaryotic DNA damage response requires the coordinated interactions between many molecular players, including damaged DNA, checkpoint proteins, chromatin, chromatin modifiers, double-stranded DNA, ssDNA, RPA, clamps, clamp loaders and kinases. Consequently, DNA damage responses are powerful intracellular pathways, which are potentially harmful for the cells; in fact, they may cause inappropriate cell cycle arrest and amplification of DNA damage if their regulation is lost. Previous work showed that chromatin modification is necessary for generating high levels of ssDNA (van Attikum *et al*, 2004). We now report the opposite role for a chromatin modification. Our findings suggest that interactions between the checkpoint protein Rad9 and methylated histone H3 inhibits ssDNA accumulation at DSBs and in response to uncapped telomeres. Tudor domains are conserved across evolution, as are methylated histone residues and we propose that Tudor domain/histone interactions may regulate resection also in other eukaryotic cell types.

Materials and methods

Strains and plasmids

Strains are listed in Supplementary Table 1. YFL399, YFL504 and YFL419 were derived from JKM179. To construct strains, standard genetic procedures of transformation and tetrad analysis were followed (Adams *et al*, 1998). YFL502 and YFL504 were obtained by integration of *Eco*RI-digested plasmid pFL37.1 at the *RAD9* locus. Pop-out events were selected on FOA plates. The Y798Q mutation in Rad9 Tudor domain was checked by PCR. Y31, Y20, Y293, YMV037, YMV038, YFL736, YFL738, YFL827, YFL809, Y28 and YFL802 derive from YMV80. Deletions and tag fusions were generated by the one-step PCR system (Longtine *et al*, 1998). Serial dilution and maximum permissive temperature analysis were performed as described (Maringele and Lydall, 2002).

Plasmid pFL36.1 was obtained by cloning a *RAD9-3HA* fragment into *Xho*I-*Not*I-digested pRS306. pFL37.1 was obtained introducing the Tudor domain mutation by site-specific mutagenesis in pFL36.1.

Microcolony assays

Cells were inoculated into 2 ml YEPD, grown overnight at 23°C until they reached saturation. The next morning, cells were sonicated briefly and plated. Plates were incubated at the indicated temperature for 20 h, photographed using a Leica DC 300F microscope and the number of cells present in 20 colonies was counted/estimated. The experiment was repeated four times, and a representative experiment is shown.

G1 block and treatment with genotoxic agents

Cells were grown in YEPD medium at 28°C to a 5×10^6 cells/ml and arrested with α-factor (10 μg/ml). Arrested cells (30 ml (untreated)) were mock treated and the rest of the culture was treated with zeocine (50 μg/ml). Treated cells (30 ml) were spun and resuspended in 20% trichloroacetic acid (TCA) for protein extract preparation at 0, 5, 10, 15 and 20 min after treatment. Cell cycle profiles were analysed by standard flow cytometry.

SDS–PAGE and western blot

TCA protein extract was prepared (Muzi-Falconi *et al*, 1993) and separated by SDS–PAGE. Western blotting was performed with anti-Rad53, anti-HA (12CA5) or anti-tubulin antibodies using standard techniques. Quantification was obtained with a Typhoon after incubation with fluorescent secondary antibodies.

Analysis of Rad53 phosphorylation levels in cdc13-1 cells

Saturated cultures grown at 23°C were diluted to 8×10^6 cells/ml and allowed to double to 1.6×10^7 cells before incubation at 28°C or 36°C for a further 5 h. A control culture was grown in parallel at 23°C. Cells were harvested, washed in H_2O and proteins were extracted with 10% TCA and solubilized in SDS–PAGE sample buffer (Blankley and Lydall, 2004). Protein samples were analysed by immunoblotting with anti-Rad53 antibody (DL58, kind gift from D Durocher).

ssDNA measurements at telomeres

ssDNA was isolated from cultures and quantified using the QAOS assay (Booth *et al*, 2001) as recently described (Zubko *et al*, 2006).

Measurement of DNA resection and SSA at DSBs

Cells grown in YEP lactate 3% medium at 28°C to a concentration of 5×10^6 cells/ml were arrested with nocodazole (20 μg/ml). A DSB was produced by adding 2% galactose and inducing the expression of the HO endonuclease. The maintenance of the arrest was confirmed by FACS analysis and monitoring of nuclear division. Genomic DNA was isolated at intervals, and the loss of the 5′ ends of the HO-cleaved *MAT* locus was determined by Southern blotting (Lee *et al*, 1998; Vaze *et al*, 2002; Clerici *et al*, 2005). All the experiments have been repeated at least three times. In the corresponding figures, one representative example is shown with its quantification.

Supplementary data

Supplementary data are available at *The EMBO Journal* Online (http://www.embojournal.org).

Acknowledgements

C Santocanale, D Durocher, K Gull, D Stern, M Clerici and MP Longhese are acknowledged for materials and reagents. M Giannattasio, F Puddu and members of DL's lab are thanked for discussions. This work was supported by grants from AIRC, Fondazione Cariplo, the European Union FP6 Integrated Project DNA repair and MIUR (to MM-F and PP). DL and VS were supported by the Wellcome Trust (075294) and CRUK (C23629/A7951). The financial support of Telethon-Italy (grant no. GGP030406 to MM-F) and research support from NIH grants GM20056 and GM61766 to JEH are gratefully acknowledged.

References

Adams A, Kaiser C, Cold Spring Harbor Laboratory (1998) *Methods in Yeast Genetics: a Cold Spring Harbor Laboratory Course Manual*. Plainview, NY: Cold Spring Harbor Laboratory Press

Aylon Y, Liefshitz B, Kupiec M (2004) The CDK regulates repair of double-strand breaks by homologous recombination during the cell cycle. *EMBO J* **23:** 4868–4875

Blankley RT, Lydall D (2004) A domain of Rad9 specifically required for activation of Chk1 in budding yeast. *J Cell Sci* **117:** 601–608

Booth C, Griffith E, Brady G, Lydall D (2001) Quantitative amplification of single-stranded DNA (QAOS) demonstrates that *cdc13-1* mutants generate ssDNA in a telomere to centromere direction. *Nucleic Acids Res* **29:** 4414–4422

Botuyan MV, Lee J, Ward IM, Kim JE, Thompson JR, Chen J, Mer G (2006) Structural basis for the methylation state-specific recognition of histone H4-K20 by 53BP1 and Crb2 in DNA repair. *Cell* **127:** 1361–1373

Caspari T, Murray JM, Carr AM (2002) Cdc2-cyclin B kinase activity links Crb2 and Rqh1-topoisomerase III. *Genes Dev* **16:** 1195–1208

Clerici M, Mantiero D, Lucchini G, Longhese MP (2005) The *Saccharomyces cerevisiae* Sae2 protein promotes resection and bridging of double strand break ends. *J Biol Chem* **280:** 38631–38638

Clerici M, Mantiero D, Lucchini G, Longhese MP (2006) The *Saccharomyces cerevisiae* Sae2 protein negatively regulates DNA damage checkpoint signalling. *EMBO Rep* **7:** 212–218

Du LL, Nakamura TM, Russell P (2006) Histone modification-dependent and -independent pathways for recruitment of checkpoint protein Crb2 to double-strand breaks. *Genes Dev* **20:** 1583–1596

Elledge SJ (1996) Cell cycle checkpoints: preventing an identity crisis. *Science* **274:** 1664–1672

Foster SS, Zubko MK, Guillard S, Lydall D (2006) MRX protects telomeric DNA at uncapped telomeres of budding yeast *cdc13-1* mutants. *DNA Repair (Amst)* **5:** 840–851

Gardner R, Putnam CW, Weinert T (1999) RAD53, DUN1 and PDS1 define two parallel G2/M checkpoint pathways in budding yeast. *EMBO J* **18:** 3173–3185

Garvik B, Carson M, Hartwell L (1995) Single-stranded DNA arising at telomeres in cdc13 mutants may constitute a specific signal for the RAD9 checkpoint. *Mol Cell Biol* **15:** 6128–6138

Giannattasio M, Lazzaro F, Plevani P, Muzi-Falconi M (2005) The DNA damage checkpoint response requires histone H2B ubiquitination by Rad6-Bre1 and H3 methylation by Dot1. *J Biol Chem* **280:** 9879–9886

Gilbert CS, Green CM, Lowndes NF (2001) Budding yeast Rad9 is an ATP-dependent Rad53 activating machine. *Mol Cell* **8:** 129–136

Grenon M, Costelloe T, Jimeno S, O'Shaughnessy A, Fitzgerald J, Zgheib O, Degerth L, Lowndes NF (2007) Docking onto chromatin via the *Saccharomyces cerevisiae* Rad9 Tudor domain. *Yeast* **24:** 105–119

Hammet A, Magill C, Helerhorst J, Jackson SP (2007) Rad9 BRCT domain interaction with phosphorylated H2AX regulates the G1 checkpoint in budding yeast. *EMBO Rep* **8:** 851–857

Harrison JC, Haber JE (2006) Surviving the breakup: the DNA damage checkpoint. *Annu Rev Genet* **40:** 209–235

Huyen Y, Zgheib O, Ditullio Jr RA, Gorgoulis VG, Zacharatos P, Petty TJ, Sheston EA, Mellert HS, Stavridi ES, Halazonetis TD (2004) Methylated lysine 79 of histone H3 targets 53BP1 to DNA double-strand breaks. *Nature* **432:** 406–411

Ira G, Pellicioli A, Balijja A, Wang X, Fiorani S, Carotenuto W, Liberi G, Bressan D, Wan L, Hollingsworth NM, Haber JE, Foiani M (2004) DNA end resection, homologous recombination and DNA damage checkpoint activation require CDK1. *Nature* **431:** 1011–1017

Ivanov EL, Sugawara N, White CI, Fabre F, Haber JE (1994) Mutations in XRS2 and RAD50 delay but do not prevent mating-type switching in *Saccharomyces cerevisiae*. *Mol Cell Biol* **14:** 3414–3425

Kornbluth S, Smythe C, Newport JW (1992) *In vitro* cell cycle arrest induced by using artificial DNA templates. *Mol Cell Biol* **12:** 3216–3223

Lee SE, Bressan DA, Petrini JH, Haber JE (2002) Complementation between N-terminal *Saccharomyces cerevisiae* mre11 alleles in DNA repair and telomere length maintenance. *DNA Repair (Amst)* **1:** 27–40

Lee SE, Moore JK, Holmes A, Umezu K, Kolodner RD, Haber JE (1998) *Saccharomyces* Ku70, mre11/rad50 and RPA proteins regulate adaptation to G2/M arrest after DNA damage. *Cell* **94:** 399–409

Limbo O, Chahwan C, Yamada Y, de Bruin RA, Wittenberg C, Russell P (2007) Ctp1 is a cell-cycle-regulated protein that functions with Mre11 complex to control double-strand break repair by homologous recombination. *Mol Cell* **28:** 134–146

Lisby M, Barlow JH, Burgess RC, Rothstein R (2004) Choreography of the DNA damage response: spatiotemporal relationships among checkpoint and repair proteins. *Cell* **118:** 699–713

Llorente B, Symington LS (2004) The Mre11 nuclease is not required for 5′ to 3′ resection at multiple HO-induced double-strand breaks. *Mol Cell Biol* **24:** 9682–9694

Longhese MP, Foiani M, Muzi-Falconi M, Lucchini G, Plevani P (1998) DNA damage checkpoint in budding yeast. *EMBO J* **17:** 5525–5528

Longtine MS, McKenzie III A, Demarini DJ, Shah NG, Wach A, Brachat A, Philippsen P, Pringle JR (1998) Additional modules for versatile and economical PCR-based gene deletion and modification in *Saccharomyces cerevisiae*. *Yeast* **14:** 953–961

Lydall D, Nikolsky Y, Bishop DK, Weinert T (1996) A meiotic recombination checkpoint controlled by mitotic checkpoint genes. *Nature* **383:** 840–843

Lydall D, Weinert T (1995) Yeast checkpoint genes in DNA damage processing: implications for repair and arrest. *Science* **270:** 1488–1491

Lydall D, Whitehall S (2005) Chromatin and the DNA damage response. *DNA Repair (Amst)* **4:** 1195–1207

Majka J, Niedziela-Majka A, Burgers PM (2006) The checkpoint clamp activates Mec1 kinase during initiation of the DNA damage checkpoint. *Mol Cell* **24:** 891–901

Maringele L, Lydall D (2002) EXO1-dependent single-stranded DNA at telomeres activates subsets of DNA damage and spindle checkpoint pathways in budding yeast yku70Delta mutants. *Genes Dev* **16:** 1919–1933

Melo J, Toczyski D (2002) A unified view of the DNA-damage checkpoint. *Curr Opin Cell Biol* **14:** 237–245

Moreau S, Ferguson JR, Symington LS (1999) The nuclease activity of Mre11 is required for meiosis but not for mating type switching, end joining, or telomere maintenance. *Mol Cell Biol* **19:** 556–566

Muzi-Falconi M, Piseri A, Ferrari M, Lucchini G, Plevani P, Foiani M (1993) *De novo* synthesis of budding yeast DNA polymerase alpha and POL1 transcription at the G1/S boundary are not required for entrance into S phase. *Proc Natl Acad Sci USA* **90:** 10519–10523

Nyberg KA, Michelson RJ, Putnam CW, Weinert TA (2002) Toward maintaining the genome: DNA damage and replication checkpoints. *Annu Rev Genet* **36:** 617–656

Paciotti V, Clerici M, Lucchini G, Longhese MP (2000) The checkpoint protein Ddc2, functionally related to *S. pombe* Rad26, interacts with Mec1 and is regulated by Mec1-dependent phosphorylation in budding yeast. *Genes Dev* **14:** 2046–2059

Rouse J, Jackson SP (2000) *LCD1*: an essential gene involved in checkpoint control and regulation of the *MEC1* signalling pathway in *Saccharomyces cerevisiae*. *EMBO J* **19:** 5801–5812

Rouse J, Jackson SP (2002) Interfaces between the detection, signaling, and repair of DNA damage. *Science* **297:** 547–551

Sanchez Y, Desany BA, Jones WJ, Liu Q, Wang B, Elledge SJ (1996) Regulation of RAD53 by the ATM-like kinases MEC1 and TEL1 in yeast cell cycle checkpoint pathways. *Science* **271:** 357–360

Sanders SL, Portoso M, Mata J, Bahler J, Allshire RC, Kouzarides T (2004) Methylation of histone H4 lysine 20 controls recruitment of Crb2 to sites of DNA damage. *Cell* **119:** 603–614

Sartori AA, Lukas C, Coates J, Mistrik M, Fu S, Bartek Baer R, Lukas J, Jackson SP (2007) Human CtIP promotes DNA end resection. *Nature* **450:** 509–514

Shroff R, Arbel-Eden A, Pilch D, Ira G, Bonner WM, Petrini JH, Haber JE, Lichten M (2004) Distribution and dynamics of chromatin modification induced by a defined DNA double-strand break. *Curr Biol* **14:** 1703–1711

Sugawara N, Ira G, Haber JE (2000) DNA length dependence of the single-strand annealing pathway and the role of *Saccharomyces cerevisiae* RAD59 in double-strand break repair. *Mol Cell Biol* **20:** 5300–5309

Sweeney FD, Yang F, Chi A, Shabanowitz J, Hunt DF, Durocher D (2005) *Saccharomyces cerevisiae* Rad9 acts as a Mec1 adaptor to allow Rad53 activation. *Curr Biol* **15:** 1364–1375

Toh GW, O'Shaughnessy AM, Jimeno S, Dobbie IM, Grenon M, Maffini S, O'Rorke A, Lowndes NF (2006) Histone H2A phosphorylation and H3 methylation are required for a novel Rad9 DSB repair function following checkpoint activation. *DNA Repair (Amst)* **5:** 693–703

Ubersax JA, Woodbury EL, Quang PN, Paraz M, Blethrow JD, Shah K, Shokat KM, Morgan DO (2003) Targets of the cyclin-dependent kinase CDK1. *Nature* **425:** 859–864

Usui T, Ogawa H, Petrini JH (2001) A DNA damage response pathway controlled by Tel1 and the Mre11 complex. *Mol Cell* **7:** 1255–1266

van Attikum H, Fritsch O, Hohn B, Gasser SM (2004) Recruitment of the INO80 complex by H2A phosphorylation links ATP-dependent chromatin remodeling with DNA double-strand break repair. *Cell* **119:** 777–788

van Leeuwen F, Gafken PR, Gottschling DE (2002) Dot1p modulates silencing in yeast by methylation of the nucleosome core. *Cell* **109:** 745–756

Vaze MB, Pellicioli A, Lee SE, Ira G, Liberi G, Arbel-Eden A, Foiani M, Haber JE (2002) Recovery from checkpoint-mediated arrest after repair of a double-strand break requires Srs2 helicase. *Mol Cell* **10:** 373–385

Vodenicharov MD, Wellinger RJ (2006) DNA degradation at unprotected telomeres in yeast is regulated by the CDK1 (Cdc28/Clb) cell-cycle kinase. *Mol Cell* **24:** 127–137

Wakayama T, Kondo T, Ando S, Matsumoto K, Sugimoto K (2001) Pie1, a protein interacting with Mec1, controls cell growth and checkpoint responses in *Saccharomyces cerevisiae*. *Mol Cell Biol* **21:** 755–764

Weinert TA, Kiser GL, Hartwell LH (1994) Mitotic checkpoint genes in budding yeast and the dependence of mitosis on DNA replication and repair. *Genes Dev* **8:** 652–665

White CI, Haber JE (1990) Intermediates of recombination during mating type switching in *Saccharomyces cerevisiae*. *EMBO J* **9:** 663–673

Wysocki R, Javaheri A, Allard S, Sha F, Cote J, Kron SJ (2005) Role of Dot1-dependent histone H3 methylation in G1 and S phase DNA damage checkpoint functions of Rad9. *Mol Cell Biol* **25:** 8430–8443

Zou L, Elledge SJ (2003) Sensing DNA damage through ATRIP recognition of RPA–ssDNA complexes. *Science* **300:** 1542–1548

Zou L, Liu D, Elledge SJ (2003) Replication protein A-mediated recruitment and activation of Rad17 complexes. *Proc Natl Acad Sci USA* **100:** 13827–13832

Zubko MK, Guillard S, Lydall D (2004) Exo1 and Rad24 differentially regulate generation of ssDNA at telomeres of *Saccharomyces cerevisiae cdc13-1* mutants. *Genetics* **168:** 103–115

Zubko MK, Maringele L, Foster SS, Lydall D (2006) Detecting repair intermediates *in vivo*: effects of DNA damage response genes on single-stranded DNA accumulation at uncapped telomeres in budding yeast. *Methods Enzymol* **409:** 285–300

